Muscle synergy analysis of short-term adaptation to arm-support exoskeletons during pseudo-static and dynamic overhead tasks

Hanjun Park[1], Maury A. Nussbaum[2]

[1]Department of Industrial, Manufacturing, and Systems Engineering, Texas Tech University, Lubbock, TX, USA

[2]Department of Industrial and Systems Engineering, Virginia Tech, Blacksburg, VA, USA

*Corresponding Author:

Hanjun Park, PhD, Texas Tech University

Lubbock, Texas, United States.

Email: hanjpark@ttu.edu

Phone: (540) 998-4325

Word count (from “Introduction” to “Conclusions): **3899**, Word count (abstract): **228**

Abstract

Occupational arm-support exoskeletons (ASEs) can reduce shoulder muscle activity during overhead work, but their effects on muscle synergy structure and temporal activation remain limited. We examined the effects of using three different exoskeletons on muscle synergies during simulated overhead tasks. Muscle activity from 18 participants (gender-balanced) performing both pseudo-static and dynamic tasks across 24 conditions (three ASEs and a control condition) was analyzed using nonnegative matrix factorization to extract synergy number, structure, and activation coefficients. Dynamic tasks recruited more muscle synergies (interquartile range: 2–5) than pseudo-static tasks (interquartile range: 1–3), with some task combinations showing modest increases with ASE use compared to control condition. Synergy structure and temporal activation were generally similar across interventions (mean cosine similarity 0.74–0.99), but certain ASE-task combinations produced significant local changes in synergy structure. Using exoskeletons generally altered muscle weightings, shifting from primary arm-elevating and shoulder-stabilizing muscles toward modules involving neck and back muscles, suggesting compensatory strategies for device-imposed biomechanical demands. Activation time courses remained highly similar across most interventions during pseudo-static tasks, though dynamic tasks showed reduced peak magnitude with exoskeleton use. Our results indicate that while modular motor control is largely preserved with ASE use, device- and task-specific adaptations in synergy structure and temporal activation can occur. Future research should explore how ASE design features influence neuromuscular strategies and assess long-term adaptation of muscle synergies in occupational settings.

Keywords: Muscle Recruitment and Coordination, Adaptation, Motor Control, Non-Negative Matrix Factorization, Human-Robot Interaction

1. Introduction

Occupational arm-support exoskeletons (ASEs) provide assistive force/torque at the proximal upper extremity, offering the potential to help address the continuing problem of work-related musculoskeletal disorders. For example, numerous studies have indicated that ASEs decrease activity in the deltoid muscles during overhead work, but also that such effectiveness varies between specific devices and tasks (Brunner et al., 2023; De Bock et al., 2020; Ojelade et al., 2023). Most reports, though, have focused on a limited set of shoulder muscle groups, assuming similar neuromuscular coordination with versus without ASEs. Furthermore, reliance on summary metrics such as mean or peak values likely does not fully capture the detailed recruitment and coordination of specific muscle groups or more general motor control strategies. A more comprehensive analysis of neuromuscular coordination could help to better understand the biomechanical and neuromuscular implications of ASEs in occupational settings.

Quantifying muscle synergies can help to understand how the central nervous system (CNS) simplifies movement control by activating predefined muscle patterns (d'Avella et al., 2003; Latash et al., 2007). The CNS uses sensory feedback and motor commands to reduce the redundancy in the musculoskeletal system through these synergies (Bruton & O'Dwyer, 2018; Latash et al., 2007). Common methods to extract synergies include principal component analysis, independent component analysis, and nonnegative matrix factorization (NMF). The latter is most typical, due to the nonnegative nature of muscle activation signals (Bruton & O'Dwyer, 2018). For example, NMF has been applied to examine both simple (e.g., elbow and shoulder flexion) and complex (e.g., overhead reaching and shoulder press) upper limb motions (Pan et al., 2021; Saito et al., 2023).

Performing tasks with an exoskeleton can alter the mechanical demands of movement by

offloading limb weight, redistributing torques across joints, and modifying proprioceptive and tactile feedback. These changes may trigger reorganization of muscle synergy structure or activation timing as the CNS adapts to altered limb dynamics and interaction forces (Coscia et al., 2014; Jacobs et al., 2018; Steele et al., 2017; Tan et al., 2019). Such adaptations likely indicate compensatory neural strategies that maintain task performance under novel assistive conditions, or motor adaptation (Izawa et al., 2008; Krakauer et al., 2019). examining motor adaptation to ASEs can be applied to enhance exoskeleton control design, guide user training, and support strategies to promote efficient human–exoskeleton interactions. However, most prior research has focused on single device types and simple cyclic or symmetric tasks. Given the complexity and variability of upper-limb movements, further investigation is needed to determine how different ASEs affect synergy organization across diverse task contexts.

We examined the effects of three different ASEs on muscle synergies during pseudo-static and dynamic overhead tasks that simulated diverse occupational demands. We sought to understand whether using an ASE alters muscle synergies, and whether these changes depend on the task. Our main hypothesis was that ASEs would not change the number of muscle synergies, muscle synergy structure and temporal activation during pseudo-static tasks, given the simplicity of these tasks, but would alter muscle synergies during dynamic tasks, reflecting modified motor control strategies. We also expected that ASE effects would vary by device type and task condition, extending our previous findings of device- and task-specific reductions in muscle activations with ASE use (Ojelade et al., 2023).

2. Methods

2.1. Experimental Design

Data used herein were obtained from prior studies, with details of the experimental design, procedures, ASEs, and simulated tasks previously reported (Morris et al., 2022; Ojelade et al., 2023). Full procedural details are provided in the Appendix. In brief, 18 healthy, young adults (9 males, 9 females) participated in the study. A repeated-measures design was used (Figure 1), in which participants completed 24 different task conditions, combining four levels of *Intervention* [i.e., Ekso Bionics™ EVO™ (EV), Paexo™ Shoulder V1 (PX), and ShoulderX™ V3 (SX), and ND = No Device], three levels of *Work Height* (*WH*), and two levels of *Force Direction* (*FD*).

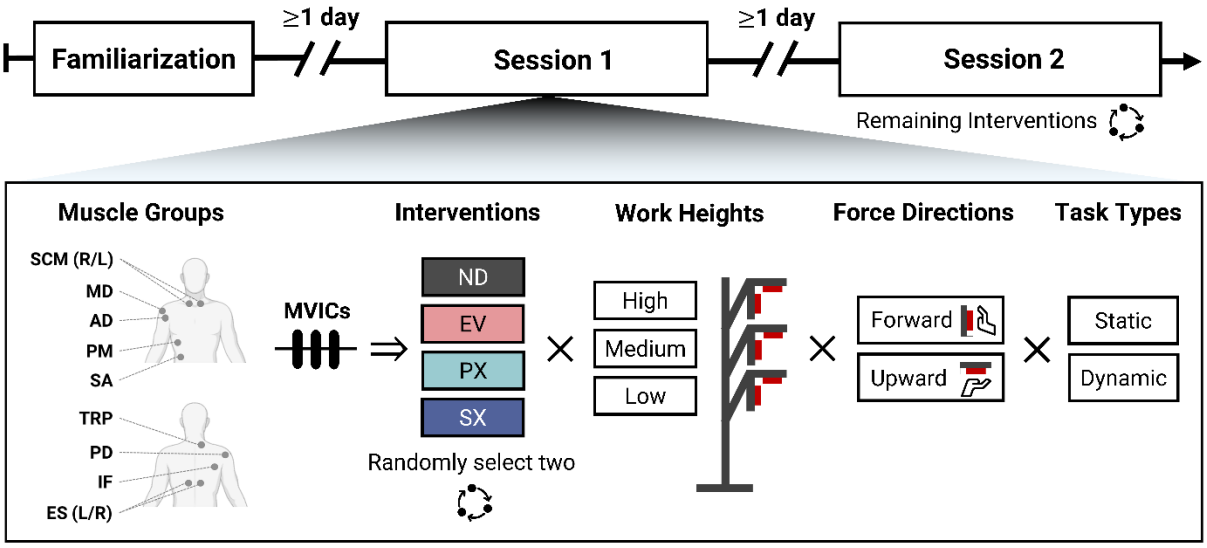

Figure 1. Overview of experimental procedures. *Interventions* included the Ekso Bionics™ EVO™ (EV), Paexo™ Shoulder V1 (PX), and ShoulderX™ V3 (SX), and ND = No Device.

Surface electromyography (EMG) was used to record the activity of 11 muscle groups using a telemetered system (TeleMyo Desktop DTS, Noraxon, AZ, USA) at 1.5 kHz. After skin preparation, pairs of Ag/AgCl EMG electrodes (with a 2.5 cm inter-electrode spacing) were placed over the target muscle groups as described by Criswell (2010). On the dominant side, the upper trapezius (TRP); anterior, middle, and posterior deltoid (AD, MD, PD); pectoralis major (PM); infraspinatus (IF); and serratus anterior (SA) were monitored, while the sternocleidomastoid (SCM)

and erector spinae (ES) were recorded bilaterally. These muscles were selected based on their relevance to the simulated overhead task and accessibility across the ASEs used (e.g., lumbar support locations and different contact areas with the body).

2.2. Muscle Synergy Analysis

Muscle synergy analysis was conducted using the following five steps (Figure 2). A custom MATLAB script was used to perform *Steps* 1–5, whereas the MATLAB function nnmf was used for implementing NMF.

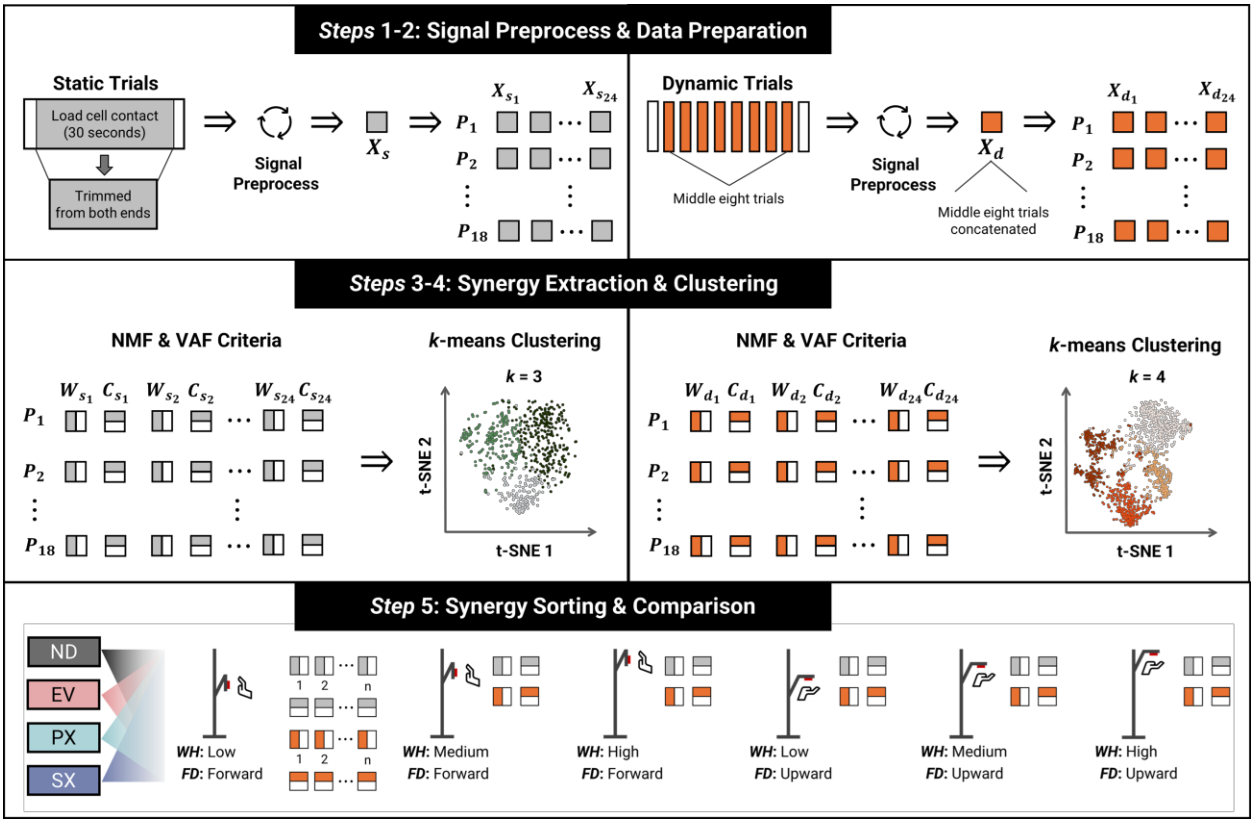

Figure 2. Overview of the muscle synergy analysis. ***Steps 1–2***: Static trials (gray) yielded single-trial EMG matrices (11×101; 24 per participant). Dynamic trials (orange) excluded the first/last repetitions; the middle eight were concatenated into one matrix (11×808; 24 per participant). In total, 48 EMG matrices were obtained per participant. ***Steps 3–4***: Each EMG matrix was decomposed via NMF into synergy weightings (W) and activation coefficients (C), yielding 432 W and 432 C matrices per task. Synergy number was determined by global (≥90%) and local (≥75%) VAF criteria. W and C were clustered using k-means and visualized with t-SNE. ***Step 5***:

Synergies were sorted and compared across *Work Height* (*WH*), *Force Direction* (*FD*), and *Intervention* conditions.

Step 1: EMG Signal Preprocessing

Raw EMG signals were high-pass filtered at 40 Hz using a zero-lag 4th order Butterworth filter, then demeaned and rectified. Processed signals were subsequently smoothed using a zero-lag, 4th-order, low-pass, Butterworth filter at 4 Hz to create a linear envelope (Clark et al., 2010). For the pseudo-static tasks, we extracted values from the 30-second period of each trial during which the exerted forces remained within the target range. The first and last three seconds of this period were trimmed to exclude muscle activation related to raising and lowering the arm, focusing the analysis on motor control relevant to the static phase. For the dynamic tasks, the first and last trials were excluded from the 10 total per condition, to minimize potential noise associated with trial initiation and termination.

Step 2: EMG Matrix Preparation

Each processed EMG signal was normalized to the corresponding maximum value recorded during maximum voluntary isometric contractions (Ojelade et al., 2023), and each trial was then time-normalized to 101 points (i.e., 0–100% of the task duration). For pseudo-static tasks, each trial yielded an $m = 11 \text{ muscles} \times t = 101 \text{ time points}$ EMG matrix, denoted as X_s; there were a total of 432 such matrices (18 participants $\times$ 3 *WH* $\times$ 2 *FD* $\times$ 4 *Intervention*). For dynamic tasks, we concatenated the middle eight trials, rather than averaging them, to preserve trial-to-trial variability (McDonald et al., 2021). Thus, t consisted of 808 points per EMG matrix for dynamic tasks, denoted as X_d (i.e., 11 $\times$ 808), of which there were also 432 total matrices. Three trials were missing from the dataset (≈0.3%). Since each task condition consisted of a single trial per

participant, within-participant interpolation was not feasible. Each missing trial was therefore imputed using the mean EMG data from other participants performing the same task condition (similar to the approach used by McPherson & Dewald, 2019). A leave-one-out evaluation showed that within-participant and between-participant approaches yielded nearly identical mean squared error values, and additional analyses confirmed that this imputation did not affect the required number of synergies or our primary outcomes.

Step 3: Muscle Synergy Extraction

Each EMG matrix X was first prepared by scaling each row to unit variance to ensure equal muscle contributions during factorization (Chvatal & Ting, 2012). Next, NMF was applied to decompose X into a weight matrix W (of size $m \times n$) and an activation matrix C (of size $n \times t$), where n denotes the number of synergies. This factorization is expressed as:

$$X \approx WC + e \ , \tag{1}$$

where e is the residual. The objective was to minimize the Frobenius norm of e:

$$\min_{W \geq 0, C \geq 0} \|X - WC\|_F^2 \ , \tag{2}$$

Matrices W and C were updated using a multiplicative update rule (Lee & Seung, 1999). NMF was repeated 50 times with random initializations, and the factorization with the lowest reconstruction error was selected. Convergence required a relative change in objective function of 1×10^{-12}, or a maximum of 2,500 iterations. The number of synergies (n) was determined by requiring both a global variance-accounted-for (VAF) of at least 90% across all 11 muscle groups

and a local VAF of at least 75% for each muscle group (Chvatal & Ting, 2012; Wang et al., 2024). We did not fix n in advance, to allow for a natural emergence of motor control modules. After factorization, the initial scaling was reversed to restore the original data magnitude, and then each synergy (and its corresponding coefficients) was normalized to its maximum muscle activation (Delis et al., 2013). The relationship between the number of extracted synergies and global VAF is presented in Appendix Figure A3.

Steps 4-5: Synergy Clustering, Sorting, and Similarity Comparison

We used *k*-means clustering to sort synergies across task conditions. The optimal number of clusters was determined based on the local maximum silhouette coefficient (Lenssen & Schubert, 2024) with *k* restricted to a range of 2–10 (Figure A2 in the Appendix). Clustering was performed separately for pseudo-static and dynamic tasks, with each participant's synergy weight vector (1×11) serving as a data point (i.e., a participant contributing n synergies provided n data points). Data from all conditions within each task were combined to facilitate comparisons across ASE types and task conditions. To minimize randomness, clustering was repeated 1,000 times with randomly chosen initial medoids and the square Euclidean distance as the metric.

Clustered synergy weights (W) were then sorted based on the 24 task conditions. Corresponding synergy activation coefficients (C) were sorted accordingly. For each cluster, the major muscles were identified based on their relative importance, calculated as $\frac{W_{k,m}}{\sum_{j=1}^{M} W_{k,j}}$, where W_k is the cluster centroid vector for synergy cluster k, $W_{k,m}$ is the weight for muscle m in cluster k, and M is the total number of muscles. Cosine similarity was then calculated across interventions to quantify structural and temporal similarity within each task type, task condition,

and cluster. Note that cosine similarity has been widely used to assess changes in muscle synergy weights and timing coefficients across different conditions (Jacobs et al., 2018; Kaufmann et al., 2024; Tajik et al., 2025).

2.3. Statistical Analysis

All statistical analyses were conducted in R software (R Core Team, 2024) for a 2 (*Task Type*) × 6 (*Condition*) × 4 (*Intervention*) repeated-measures design. To assess the effect of *Task Type*, *Condition*, and *Intervention* on the number of synergies, Generalized Estimation Equation (GEE) models were fitted with a Poisson distribution, log link, and a working correlation structure clustered by participant (Zeger et al., 1988). Separate models were fit for each *Task Type* and *Condition*, with *Intervention* as a fixed effect. Proportion values of synergy types were summarized descriptively. To assess differences in muscle synergy structure and activation pattern similarity (i.e., cosine similarity) between ND and each ASE condition, linear mixed-effects models were performed separately for each *Task Type*, *Condition*, and synergy cluster. Each model included *Intervention* as a fixed effect and participant as a random effect. Planned pairwise comparisons were conducted between ND and each ASE condition. Statistical significance was set at $p < 0.05$. Due to the relatively small sample size relative to the number of task conditions, and to avoid overly conservative thresholds, *p*-values were not adjusted for multiple post-hoc comparisons.

3. Results

3.1. Number of Muscle Synergies

The number of synergies differed between *Task Type*, with pseudo-static tasks generally recruiting fewer synergies (interquartile range [IQR]: 1–3) than dynamic tasks (IQR: 2–5; Figure 3; Table

A2 in the Appendix). *Condition* also influenced synergy count. Compared to the *Low–Forward*, the *Low–Upward* condition had ~1 fewer synergy. Pairwise comparisons within specific task conditions showed some significant effects. During pseudo-static *Low–* and *Medium–Upward* conditions, SX and PX use, respectively, led to higher synergy counts compared to ND. For dynamic forward tasks, synergy counts significantly increased with SX use at all heights and with PX at medium height, compared to ND.

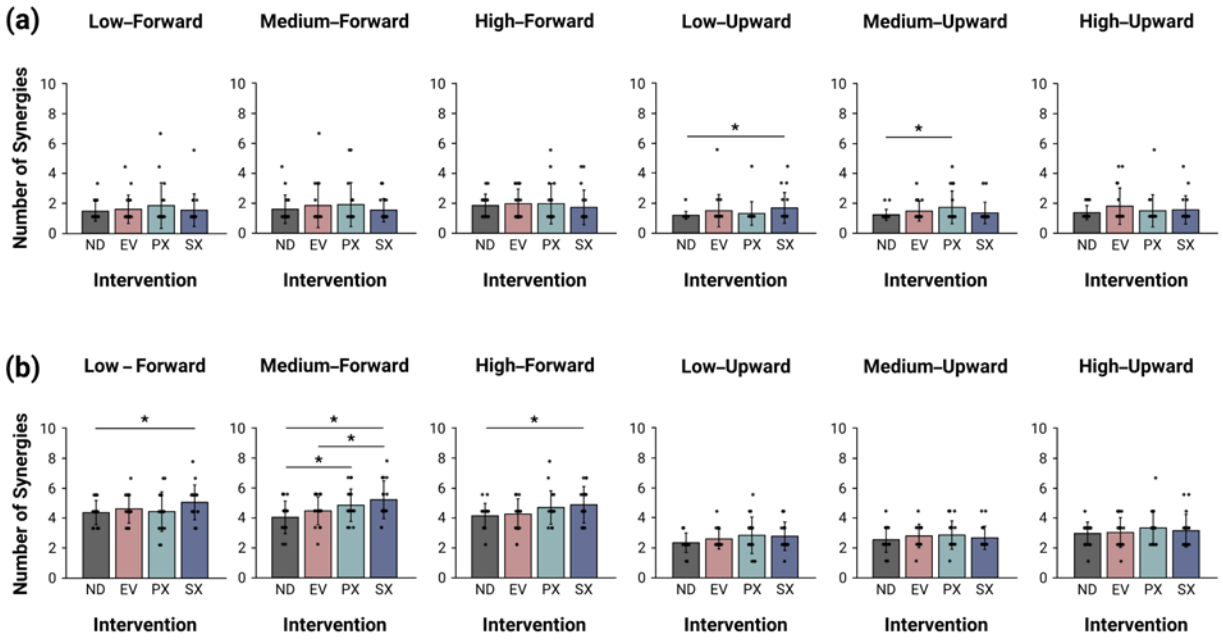

Figure 3. Number of synergies for the (a) pseudo-static and (b) dynamic tasks across *Condition* and *Intervention*. Each bar represents the mean number of synergies, with individual data shown as black dotted points and with error bars representing standard deviations. The symbol * denotes a significant paired difference between *Intervention* conditions within a specific *Condition*.

3.2. Muscle Synergy Structure

Three representative clusters were identified for pseudo-static tasks and four for dynamic tasks (Figure 4). For pseudo-static tasks, the major muscle groups in each cluster were defined as follows: Cluster 1 (AD, SA), Cluster 2 (TRP, SA), and Cluster 3 (SCM_L). For dynamic tasks, the clusters

were: Cluster 1 (AD, IF, SA), Cluster 2 (TRP, ES_L), Cluster 3 (SCM_L, PM), and Cluster 4 (ES_R, SA). While overall intervention distributions across task conditions did not differ substantially, the proportions varied. In pseudo-static low height conditions, for example, Cluster 3 included no synergies associated with ND condition; in dynamic tasks, ND synergies were more frequent in Clusters 1 and 2 (mean proportion of 28%), and less frequent in Clusters 3 and 4 (mean proportion of 19%).

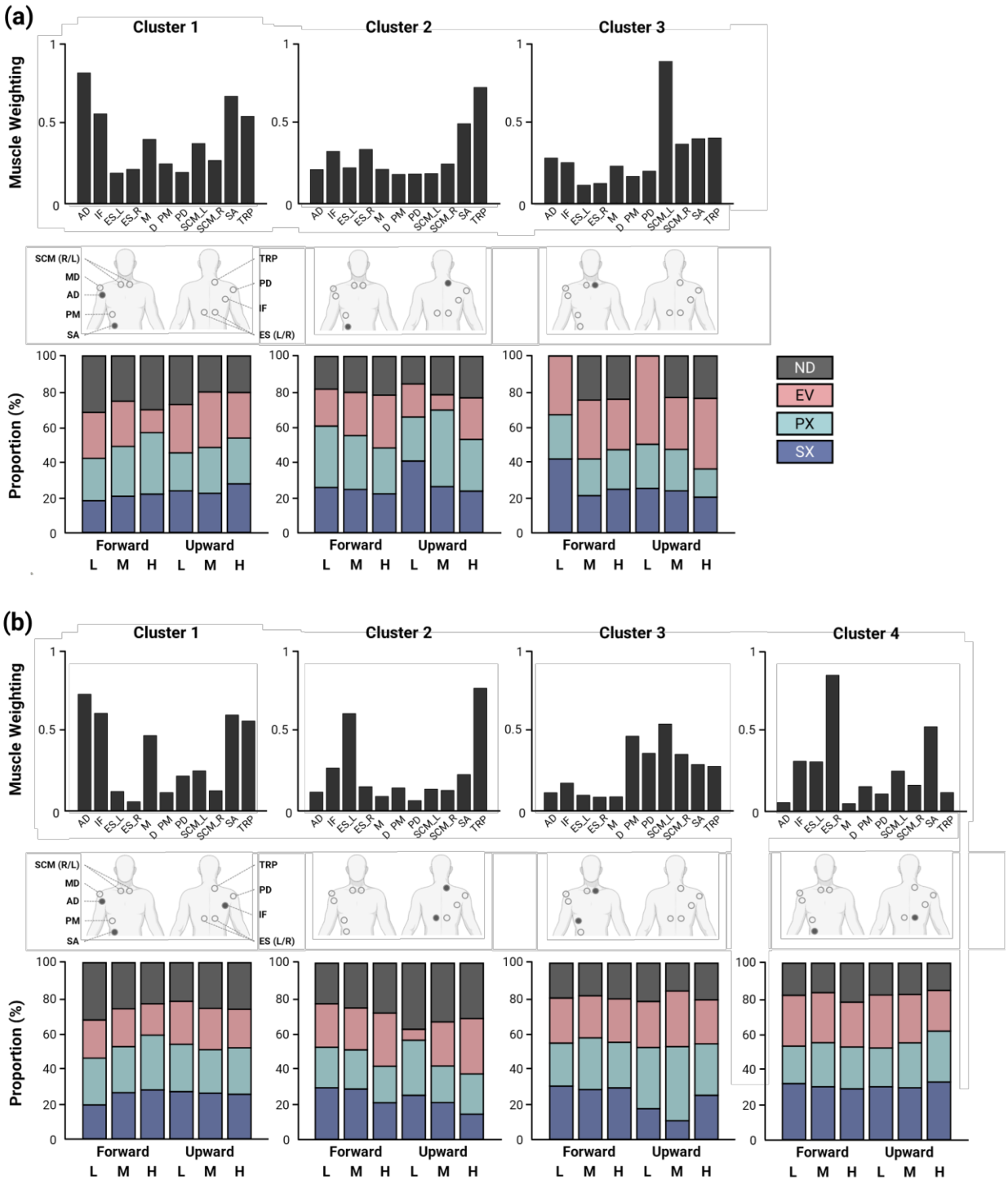

Figure 4. Muscle synergy analysis clustering results for (a) pseudo-static and (b) dynamic tasks. In each panel, the top bar graph shows the mean muscle weightings for 11 muscle groups within each cluster, with major contributors highlighted in grey (middle). The bottom stacked bar plots indicate the proportion of synergies associated with different *Interventions* and *Conditions* (L: *Low*, M: *Medium*, H: *High WH*).

For both pseudo-static and dynamic tasks, synergy weight structures were generally consistent across interventions, with mean (SD) cosine similarity values ranging from 0.74 (0.04) to 0.92 (0.17) in pseudo-static tasks and 0.69 (0.06) to 0.90 (0.24) in dynamic tasks (Figure 5; Tables A3-A4 in the Appendix). However, significant differences between ND and ASEs (EV, PX, SX) emerged in specific cluster-condition combinations. In *Low–Forward* Cluster 1, all assistive devices caused significantly different synergy structures compared to ND. Notably, wearing the SX resulted in consistently altered synergy structures in *Medium–Forward*, *Low–*, and *Medium-Upward* tasks within Cluster 1. In contrast, dynamic tasks showed no significant differences across interventions in *Low–Forward* Cluster 1. Larger differences between ND and the assistive devices emerged in Clusters 3 and 4 during dynamic tasks. In Cluster 3, PX and SX significantly differed from ND in *Medium–Forward*, and PX differed significantly in the *High–Upward* condition. In Cluster 4, PX and SX led to significant differences in most upward task conditions.

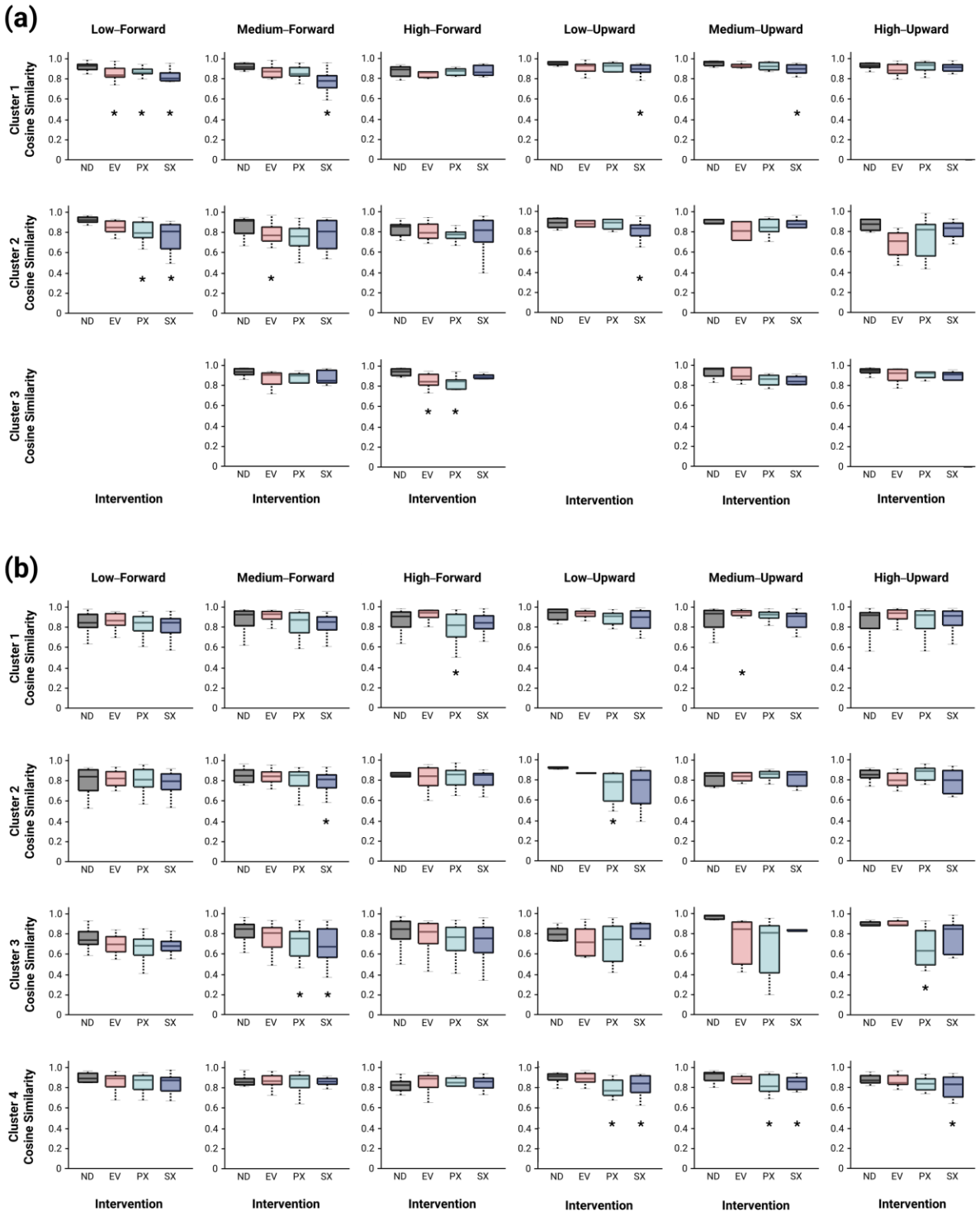

Figure 5. Synergy **weight** similarity for (a) pseudo-static and (b) dynamic tasks across conditions and clusters. Cosine similarity (y-axis) is shown by *Intervention* (x-axis). The '*' symbol indicates significant differences between ND and ASEs. ND mean similarity was computed against group-mean synergies (Vergara-Diaz et al., 2025).

3.3. Muscle Synergy Timing (Activation Coefficients)

Cosine similarity of timing coefficients across *Interventions* within each task condition were consistently high in both the pseudo-static and dynamic tasks (Figures A4-A5; Tables A5-A6 in the Appendix). However, pseudo-static tasks exhibited slightly higher similarity compared to dynamic tasks, with a mean cosine similarity of 0.90–0.99 vs. 0.77–0.93 for dynamic task conditions. In pseudo-static tasks, most interventions showed no significant differences from the ND across clusters and task conditions. A few exceptions include a significant reduction in timing similarity for EV in *Medium–Upward* Cluster 2, and for SX in *Medium–Upward* Cluster 3. In dynamic tasks, timing similarity was more variable. Specifically, *Medium–* and *High–Upward* Cluster 2 exhibited relatively lower mean cosine similarity values (≤0.82), reflecting greater variability in activation pattern with ASE use. Some significant intervention effects were observed, including EV and SX in *Medium–Upward* Cluster 2 and SX in *High–Upward* Cluster 2.

4. Discussion

4.1. Number of Muscle Synergies

At a broad level, the number of synergies remained stable across most interventions, indicating that short-term ASE exposure does not fundamentally alter modular control. However, dynamic tasks required more synergies (IQR: 2–5) than pseudo-static tasks (IQR: 1–3), consistent with prior findings that greater mechanical complexity increases modular recruitment (Chvatal & Ting, 2012; Ivanenko et al., 2005). Certain conditions involving specific ASEs (SX and PX) led to modest yet statistically significant increases in synergy counts compared to ND, particularly during dynamic forward tasks. For example, wearing SX increased synergy numbers during medium/high forward pushes, and PX during medium forward tasks.

To further interpret these increases, we examined cluster-level synergy composition. During forward-dynamic tasks, PX and SX exhibited higher proportions of synergies in Clusters 3 and 4 (Cluster 3: ND 18%, PX 24%, SX 30%; Cluster 4: ND 19%, PX 31%, SX 23%) than ND. These clusters primarily represented activation of neck and dominant-side back muscles, suggesting that PX and SX required additional synergies to stabilize these regions. Because all participants were right-handed, ND would be expected to show a greater proportion of Cluster 2 synergies dominated by left-sided back activation, reflecting unilateral effort during one-handed overhead tasks. In contrast, using PX and SX promoted more balanced, bilateral distribution of synergy loadings, indicating more symmetric recruitment patterns with ASE assistance.

Participants completed a familiarization session (~3 hour) prior to two subsequent experimental sessions (~3 hour each), all on separate days (Ojelade et al., 2023). Although we did not measure muscle activity during familiarization, ~3 hours of exposure was likely to have minimized initial adjustment effects and ensure relatively stable task performance. Thus, the observed synergy increases are more plausibly attributed to short-term modulation of CNS recruitment of additional motor modules to manage novel perturbations imposed by ASEs, rather than insufficient familiarization. This interpretation is supported by evidence that exoskeleton assistance altered synergy structure and reduced dominant muscle activations in response to novel biomechanical demands, as demonstrated in both walking (Jacobs et al., 2018) and squatting (Jeong et al., 2023). However, this contrasts with (Cohic et al., 2025), who found that back-support exoskeleton use increased VAF, suggesting reduced number of motor modules, although the effect was minimal (0.48%). They further noted that the VAF increase may be due to movement restrictions. Taken together, these findings suggest that exploring the relationship between synergy number and joint kinematics is warranted to more comprehensively understand ASE effects on

motor modularity.

Interestingly, we found fewer synergy increases with ASEs during dynamic upward pushes compared to forward pushes (respective mean increases of 2.5 vs. 4.1), likely because the upward-directed support from ASEs aligns more naturally with task demands, minimizing conflicts that might necessitate additional synergy recruitment. Among conditions, dynamic forward pushing likely posed the most novel perturbations due to opposing force direction and complexity, making it most challenging for motor adaptation. Recently, (Vergara-Diaz et al., 2025) similarly showed that robot-assisted gait training increased muscle synergy numbers among children with cerebral palsy, reflecting functional improvements and highlighting the CNS's adaptive capacity in response to external assistance. The modest synergy increases we observed may indicate that adaptive CNS modulation when confronted with novel mechanical demands is a broader phenomenon.

It is also plausible that specific ASE design features (e.g., mass and support mechanisms) contributed to the variability we observed in synergy recruitment. For instance, SX and PX provide upward-directed assistance primarily through shoulder pads, potentially requiring compensatory muscle recruitment for forward-directed tasks. Future studies should investigate how specific device characteristics influence synergy modulation across diverse tasks.

4.2. Muscle Synergy Structure

The distribution of muscle synergies varied substantially by *Intervention* and *Condition*. In pseudo-static low height conditions, the synergy cluster representing neck musculature (Cluster 3) was absent in the ND condition, while ASE use caused more uniform recruitment of neck muscle synergies across conditions. These outcomes may reflect increased neck muscle stiffness or

compensatory co-contraction or simply altered coordination strategies necessitated by the physical constraints of ASEs. Our earlier EMG analysis (Ojelade et al., 2023) demonstrated that ASE use generally reduced SCM activation. Previous studies also indicate that neck flexion or extension typically increases SCM activation (e.g., Cheon & Park, 2017; Ng et al., 2014; Nimbarte et al., 2012). Since low-height task conditions do not require substantial deviations from neutral neck postures, differences in synergy distribution within Cluster 3 for ND vs. ASE conditions likely reflect altered motor coordination strategies and reorganization of muscle groupings, rather than increased neck muscle activation with ASE use. Caution is warranted, however, because no direct kinematic data were collected to support this interpretation.

During dynamic tasks, synergy distributions for Clusters 1–4 were more evenly balanced across ASE conditions vs. ND. In the ND condition, a higher proportion of synergies were associated with the primary arm-elevating and shoulder-stabilizing muscles (i.e., AD, TRP, LES), suggesting greater reliance on these muscles without assistive support. In contrast, using ASEs shifted synergy recruitment to modules involving neck and back muscles (Clusters 3 and 4), possibly reflecting compensatory motor strategies in response to ASE mechanical demands and support characteristics. Future studies assessing both muscle synergy and EMG analyses over extended adaptation periods are needed to better understand these neuromuscular reorganizations.

Within clusters, synergy weight similarity was generally high across interventions, though specific pairs of interventions had important structural differences. Specifically, using the SX caused the most frequent alterations in synergy structure across low and medium task heights, whereas outcomes using PX and SX diverged most from ND during dynamic upward tasks (notably in Cluster 4). These findings may stem from the distinct mechanical designs and support mechanisms of each ASE. As examples: 1) the coil spring and cable mechanisms of SX and PX

likely impose biomechanical demands different from the gas spring system of EV, perhaps requiring more complex local adaptations; and 2) device mass, padding, and support level adjustability (Figure A1 in the Appendix) could account for the observed variability in synergy adaptation. We encourage additional work to link ASE design parameters with neuromuscular control strategies.

4.3. Muscle Timing (Activation Coefficients)

Timing coefficient patterns remained generally consistent across *Interventions*, with high cosine similarity values in both pseudo-static (0.90–0.99) and dynamic (0.77–0.93) tasks. However, timing similarity was slightly lower and more variable in dynamic tasks, suggesting that the temporal organization of muscle activations is more robust during less mechanically demanding, pseudo-static tasks. While activation patterns were mostly similar, the absolute magnitude of timing coefficients differed substantially between ND and ASE conditions, especially during upward pushing in both pseudo-static and dynamic tasks. Our secondary analysis showed that the mean peak timing coefficient in Cluster 1 and 2 was up to ~35% and ~55% larger when using ASEs vs. ND during pseudo-static and dynamic tasks, respectively. Larger timing coefficients do not always equate to increases in individual muscle activation. Yet, it does indicate greater recruitment of the synergy at specific time points, particularly relevant for Clusters 1 and 2, which represent muscles responsible for arm elevation and shoulder stabilization (AD, TRP, LES). This interpretation is also supported by our previous finding (Ojelade et al., 2023) that using ASEs typically reduced AD, TRP, and LES activation.

Several intervention-task pairs also reduced timing similarity. In pseudo-static tasks, EV lowered similarity in *High–Upward* Cluster 1 and *Medium-Upward* Cluster 2. During dynamic

tasks, similarity for ND vs. ASEs decreased below 0.82 for *Medium–* and *High–Upward* conditions in Cluster 2, suggesting larger temporal adjustments. Prior work likewise showed flexible modulation of synergy timing in response to novel mechanical constraints or perturbations (Jacobs et al., 2018; Steele et al., 2017). Together, these results suggest that exoskeleton assistance imposes novel biomechanical demands, requiring the CNS to adjust what muscles are recruited and during short-term ASE exposure.

5. Limitations

Several limitations should be acknowledged. First, we employed a relatively small and homogenous sample, so generalizability to a broader population is unclear. Second, we could not assess longer-term effects of motor adaptation, since participants completed only one trial per task following a short familiarization session. Although all participants practiced until they felt comfortable, the limited exposure may not have allowed muscle synergy patterns to stabilize. Future studies should use multi-session or longitudinal designs to examine how neuromuscular strategies evolve and whether early additional synergies diminish with experience. Third, our results may be sensitive to the selected thresholds for VAF. Although our choices were consistent with prior reports (e.g., Jacobs et al., 2018; Vergara-Diaz et al., 2025), small differences could influence the number of extracted synergies. Fourth, although we qualitatively assessed potential influences of device-specific features on muscle synergy, these factors were not explicitly quantified. Future studies should systematically evaluate how such design characteristics contribute to neuromuscular coordination differences across exoskeletons. Fifth, although missing EMG data were minimal (≈0.3%,) and our additional analyses confirmed that imputation did not alter our main outcomes, more advanced approaches (e.g., nearest-neighbor, linear interpolation,

or multiple imputation) would be warranted when greater missingness is present or when replications are available. Lastly, since direct kinematic or kinetic data were not collected, interpretations of synergy structure and timing coefficients should be viewed as indicative of altered coordination rather than confirmed changes in movement mechanics.

6. Conclusions

We found that using ASEs induced modest alterations to both muscle synergy structure and activation pattern, with the magnitude of effects depending on synergy cluster, task type, and condition. More synergies were required during dynamic vs. pseudo-static tasks, and certain ASEs caused greater deviations from baseline (ND) motor strategies. ASEs use induced neck muscle-related synergies during pseudo-static low-height tasks, possibly reflecting unintended neck recruitment under these conditions. In contrast, shoulder and back muscle recruitment and activation pattern were substantially reduced with ASE use during dynamic tasks, indicating more efficient neuromuscular coordination of the arm and shoulder musculature, consistent with the effective assistance reported previously (Ojelade et al., 2023), albeit with possible tradeoffs in neck activation due to device constraints. Our results highlight the importance of considering both biomechanical and ergonomic factors in ASE design. Longitudinal studies are warranted to determine whether initial synergy adaptations consolidate into stable motor patterns with extended ASE use or revert to baseline following adaptation.

Acknowledgement

The first author was supported by a pre-doctoral training program grant (T03 OH008613) from the U.S. Centers for Disease Control and Prevention. The contents of this work are solely the responsibility of the authors and do not necessarily represent the official views of the Centers for Disease Control and Prevention or the Department of Health and Human Services.

References

Brunner, A., van Sluijs, R., Luder, T., Camichel, C., Kos, M., Bee, D., Bartenbach, V., Lambercy, O., 2023. Effect of passive shoulder exoskeleton support during working with arms over shoulder level. Wearable Technol. 4, e26.

Bruton, M., O'Dwyer, N., 2018. Synergies in coordination: a comprehensive overview of neural, computational, and behavioral approaches. J. Neurophysiol. 120, 2761–2774.

Cheon, S.H., Park, S.H., 2017. Changes in neck and upper trunk muscle activities according to the angle of movement of the neck in subjects with forward head posture. J. Phys. Ther. Sci. 29, 191–193. https://doi.org/10.1589/jpts.29.191

Chvatal, S.A., Ting, L.H., 2012. Voluntary and reactive recruitment of locomotor muscle synergies during perturbed walking. J. Neurosci. 32, 12237–12250.

Clark, D.J., Ting, L.H., Zajac, F.E., Neptune, R.R., Kautz, S.A., 2010. Merging of healthy motor modules predicts reduced locomotor performance and muscle coordination complexity post-stroke. J. Neurophysiol. 103, 844–857. https://doi.org/10.1152/jn.00825.2009

Cohic, A., Segers, T., Thamsuwan, O., 2025. Impact of an occupational back-support exoskeleton on muscle synergies during a pick-up movement. Eur. J. Appl. Physiol. 1-16. https://doi.org/10.1007/s00421-025-05954-4

Coscia, M., Cheung, V.C.K., Tropea, P., Koenig, A., Monaco, V., Bennis, C., Micera, S., Bonato, P., 2014. The effect of arm weight support on upper limb muscle synergies during reaching movements. J. Neuroengineering Rehabil. 11, 1–15.

d'Avella, A., Saltiel, P., Bizzi, E., 2003. Combinations of muscle synergies in the construction of a natural motor behavior. Nat. Neurosci. 6, 300–308.

De Bock, S., Ghillebert, J., Govaerts, R., Elprama, S.A., Marusic, U., Serrien, B., Jacobs, A., Geeroms, J., Meeusen, R., De Pauw, K., 2020. Passive shoulder exoskeletons: More effective in the lab than in the field? IEEE Trans. Neural Syst. Rehabil. Eng. 29, 173–183.

Delis, I., Berret, B., Pozzo, T., Panzeri, S., 2013. Quantitative evaluation of muscle synergy models: A single-trial task decoding approach. Front. Comput. Neurosci. 7, 8. https://doi.org/10.3389/fncom.2013.00008

Ivanenko, Y.P., Cappellini, G., Dominici, N., Poppele, R.E., Lacquaniti, F., 2005. Coordination of locomotion with voluntary movements in humans. J. Neurosci. 25, 7238–7253. https://doi.org/10.1523/JNEUROSCI.1327-05.2005

Izawa, J., Rane, T., Donchin, O., Shadmehr, R., 2008. Motor adaptation as a process of reoptimization. J. Neurosci. 28, 2883–2891. https://doi.org/10.1523/JNEUROSCI.5359-07.2008

Jacobs, D.A., Koller, J.R., Steele, K.M., Ferris, D.P., 2018. Motor modules during adaptation to walking in a powered ankle exoskeleton. J. NeuroEngineering Rehabil. 15, 2. https://doi.org/10.1186/s12984-017-0343-x

Jeong, H., Haghighat, P., Kantharaju, P., Jacobson, M., Jeong, H., Kim, M., 2023. Muscle coordination and recruitment during squat assistance using a robotic ankle–foot exoskeleton. Sci. Rep. 13, 1–10. https://doi.org/10.1038/s41598-023-28229-4

Kaufmann, P., Zweier, L., Baca, A., Kainz, H., 2024. Muscle synergies are shared across fundamental subtasks in complex movements of skateboarding. Sci. Rep. 14, 1–14. https://doi.org/10.1038/s41598-024-63640-5

Krakauer, J.W., Hadjiosif, A.M., Xu, J., Wong, A.L., Haith, A.M., 2019. Motor learning. Compr. Physiol. 9, 613–663. https://doi.org/10.1002/cphy.c170043

Latash, M.L., Scholz, J.P., Schöner, G., 2007. Toward a new theory of motor synergies. Motor Control 11, 276–308. https://doi.org/10.1123/mcj.11.3.276

Lee, D.D., Seung, H.S., 1999. Learning the parts of objects by non-negative matrix factorization. Nature 401, 788–791.

Lenssen, L., Schubert, E., 2024. Medoid Silhouette clustering with automatic cluster number selection. Inf. Syst. 120, 102290.

McDonald, C.G., Fregly, B.J., O'Malley, M.K., 2021. Effect of robotic exoskeleton motion constraints on upper limb muscle synergies: A case study. IEEE Trans. Neural Syst. Rehabil. Eng. 29, 2086–2095. https://doi.org/10.1109/TNSRE.2021.3118591

McPherson, L.M., Dewald, J.P.A., 2019. Differences between flexion and extension synergy-driven coupling at the elbow, wrist, and fingers of individuals with chronic hemiparetic stroke. Clin. Neurophysiol. 130, 454–468. https://doi.org/10.1016/j.clinph.2019.01.010

Morris, W., Kim, S., Ojelade, A., Srinivasan, D., Smets, M., Nussbaum, M.A., 2022. Subjective assessments of arm-support exoskeletons during simulated static and dynamic overhead tasks. Proceedings of the Human Factors and Ergonomics Society Annual Meeting 66, 266-267. https://doi.org/10.1177/1071181322661227

Ng, D., McNee, C., Kieser, J., Farella, M., 2014. Neck and shoulder muscle activity during standardized work-related postural tasks. Appl. Ergon. 45, 556–563. https://doi.org/10.1016/j.apergo.2013.07.012

Nimbarte, A.D., Aghazadeh, F., Ikuma, L., Sun, Y., 2012. Evaluation of the loading of neck and shoulder musculature in overhead pushing and pulling exertions. Hum. Factors Ergon. Manuf. 22, 317–327. https://doi.org/10.1002/hfm.20283

Ojelade, A., Morris, W., Kim, S., Kelson, D., Srinivasan, D., Smets, M., Nussbaum, M.A., 2023. Three passive arm-support exoskeletons have inconsistent effects on muscle activity, posture, and perceived exertion during diverse simulated pseudo-static overhead nutrunning tasks. Appl. Ergon. 110, 104015. https://doi.org/10.1016/j.apergo.2023.104015.

Pan, C., Lu, M., Xu, B., 2021. An empirical study on software defect prediction using codebert model. Appl. Sci. Switz. 11, 4793. https://doi.org/10.3390/app11114793

Saito, H., Yokoyama, H., Sasaki, A., Matsushita, K., Nakazawa, K., 2023. Variability of trunk muscle synergies underlying the multidirectional movements and stability trunk motor tasks in healthy individuals. Sci. Rep. 13, 1–12. https://doi.org/10.1038/s41598-023-28467-6

Steele, K.M., Jackson, R.W., Shuman, B.R., Collins, S.H., 2017. Muscle recruitment and coordination with an ankle exoskeleton. J. Biomech. 59, 50–58. https://doi.org/10.1016/j.jbiomech.2017.05.010

Tajik, R., Dhahbi, W., Fadaei, H., Mimar, R., 2025. Muscle synergy analysis during badminton forehand overhead smash: integrating electromyography and musculoskeletal modeling. Front. Sports Act. Living 7, 1–15. https://doi.org/10.3389/fspor.2025.1596670

Tan, C.K., Kadone, H., Miura, K., Abe, T., Koda, M., Yamazaki, M., Sankai, Y., Suzuki, K., 2019. Muscle synergies during repetitive stoop lifting with a bioelectrically-controlled lumbar support exoskeleton. Front. Hum. Neurosci. 13, 142.

Vergara-Diaz, G.P., Sapienza, S., Daneault, J.F., Fabara, E., Adans-Dester, C., Severini, G., Cheung, V.C.K., de Vargas, C.E.R., Nimec, D., Bonato, P., 2025. Can muscle synergies shed light on the mechanisms underlying motor gains in response to robot-assisted gait training in children with cerebral palsy? J. NeuroEngineering Rehabil. 22. https://doi.org/10.1186/s12984-025-01550-x

Wang, S., Purohit, R., Criekinge, T.V., Bhatt, T., 2024. Neuromuscular mechanisms of motor adaptation to repeated treadmill-slip perturbations during stance in healthy young adults. IEEE Trans. Neural Syst. Rehabil. Eng. 32, 4207–4218. https://doi.org/10.1109/TNSRE.2024.3485580

Zeger, S.L., Liang, K.-Y., Albert, P.S., 1988. Models for longitudinal data: A generalized estimating equation approach. Biometrics 44, 1049-1060.